Hindawi
Advances in Materials Science and Engineering
Volume 2018, Article ID 8130647, 13 pages
https://doi.org/10.1155/2018/8130647

Research Article

The Standard Fire Testing and Numerical Modelling of the Behavior of Calcium Silicate Board Metallic-Framework Drywall Assembly with Junction Box

Yinuo Wang,[1] **Ying-Ji Chuang**,[2] **Ching-Yuan Lin**,[2] **and Hao Zhang**[1,3]

[1]*China Academy of Building Research, Beijing 100013, China*
[2]*Department of Architecture, National Taiwan University of Science and Technology, Taipei, Taiwan*
[3]*University of Science and Technology, Beijing, China*

Correspondence should be addressed to Yinuo Wang; wyn_up@foxmail.com

Received 11 October 2017; Revised 9 April 2018; Accepted 18 April 2018; Published 4 June 2018

Academic Editor: Ana S. Guimarães

The metallic-framework drywall is used as the specimens in this research. The standard fire test and finite element simulation were performed once on 300 cm × 300 cm area specimen and twice on 100 cm × 100 cm area specimens, to quantify and evaluate the effect of the junction boxes on the fireproof property after being embedded into the metallic-framework drywall. The results of the experiment show that the temperature of unexposed surface rises faster due to the higher thermal conductivity of the internal metal junction box. The general junction box whose material is PVC can be softened off when heated, affecting the integrity of the firewall and also leading to rapid transfer to the unexposed surface. The prediction of finite element simulation temperature is highly correlated with the results of the real experiment. It is effective to strengthen the original weaknesses by adding a calcium silicate board behind the junction box and using metal panels instead of PVC. The temperature of the temperature junction box surface which is the highest temperature point of unexposed surface decreased most significantly at 72.9°C after the reinforcement. In addition, after reinforcement, the fire resistance time can reach to 1 hour by inserting the junction box into the metallic-framework drywall.

1. Introduction

With the development of architectural technology and fire engineering during the last decade, the construction project tends to develop high-rise and giant buildings. To adapt the tendency, a method of reducing the weight of the building, avoiding the construction risks and shortening the constructional duration, becomes an important issue for architectural engineering. In addition, the usage of thick and heavy building materials such as traditional brick wall or concrete wall must be reduced. For example, different dry metallic-framework wall systems which are expected to replace the traditional thick and heavy building materials appear constantly. These systems have features of optimization of construction methods, short constructional duration, and various constructional methods and light materials whose quality is more stable than concrete. With the gradual popularity of new materials and new constructional methods, such as dry metallic-framework wall system, whether they can achieve a certain time of fire resistance and can be applied in the fire division become more and more important. Whether the building components have the appropriate fire safety should be detected by the standard fire test [1–6]. In addition, they should be applied to the buildings after they are equipped with the capacity of thermal resistance or fire integrity [7]. Based on the test time, these products can be classified by the fire resistance. For example, the firewalls can be classified into 1-hour, 2-hour, or 3-hour fire resistance.

There are many investigated studies on the performance issues of the dry metallic-framework wall partitioning system. Lin et al. [8] investigated the combination of metallic framework and calcium silicate board. Ho and Tsai [9]

proposed that the quality of boards had a great effect on the fire resistance of the wall. Nithyadharan and Kalyanaraman [10] researched on the strength of the connection of screw and calcium silicate board. Chuang et al. [11] came up with the conclusion that the room temperature had a direct influence on the surface temperature when the specimen was tested for fire resistance. Maruyama et al. [12] researched the aging of calcium silicate board and found that its strength weakened as time goes by.

The above research studies on the fire resistance of dry metallic-framework wall are based on the standard fire test experiments. With CAE (computer-aided engineering) increasingly being applied in various engineering fields, as an important part of CAE, CFD (computational fluid dynamics) has been developed rapidly during the last two decades. The principle of CFD is to solve the differential equations of nonlinear simultaneous quality, energy, component, momentum, and scalar with numerical methods. The results of solutions are able to predict the details of movement, heat transmission, mass transmission, and burning, becoming an efficient tool to optimize process equipment and enlarge quantitative design. The basic features of CFD are numerical modelling and computer experiment. Beginning from the fundamental physical theorems, to a large extent, they replaced the expensive equipment for fluid dynamic experiments, greatly influencing the scientific researches and engineering technology.

CFD is mainly applied in cutting-edge designs, such as aerospace design, automobile design, and turbine design. In addition, more and more numerical simultaneous aided researches in building field are processed by making use of CFD. For example, Collier and Buchanan [13] presented the prediction model for fire resistance of drywall by the finite element method; Do et al. [14] came up with that the thermal conductivity of porous material is mainly related to the thermal conductivity of its components and spatial arrangement of its complex structure by formula, microstructure observation, and experiments; Nassif et al. [15] presented the comparison of thermal conductivity of a dry gypsum board wall by the standard fire experiment and by numerical modelling.

According to regulations in different countries or the above researches which focus on the standard fire test experiment or computer simulation, they are only studying and discussing focusing on the wall. Wang et al. [16] once proposed that installing devices, such as the embedded junction box in the wall, could influence the fire resistance of the wall. However, this research focused on the quality control of the board with standard fire test experiment. It does not consider numerical modelling and corresponding quantitative research.

Based on the above foundation, this research takes the dry metallic-framework wall with embedded junction box as the experimental specimens. The quantitative analysis of its fire resistance through a physical experiment and CFD numerical modelling gives improvement measures for its destruction behavior. Aiming at disruptive behaviors, filling the existing gaps, and supplementing the fields are not involved in regulations of various countries at present.

The research conducts a total of 3 standard fire resistance tests and numerical modelling simulations. Test 1 uses the standard of ISO 834-1 [2] to perform the test on a test specimen with a of size 300 cm (width) ∗ 300 cm (height), proposes the numerical model to simulate the process of transient heat transmission, compares the results of computer simulation and the test results, and properly optimizes the digital model parameters. In Test 2, the fire area of the specimen is 100 cm (width) ∗ 100 cm (height), and an embedded junction box in the testing specimen was used to compare the numerical modelling of CFD models. By quantitative analysis, the weakness of the embedded junction box in the wall can be analyzed, which influences the fire resistance, and the reinforcement scheme was proposed. Test 3 simulates the feasibility of the reinforcement scheme by CFD numerical modelling, tests on the specimen of which fire area is 100 cm (width) ∗ 100 cm (height), and verifies the feasibility of numerical modelling and reinforcement scheme by the use of the standard fire test.

2. Experimental Details

2.1. Fire Test Furnaces. In this research, two sets of test equipment are applied, and both can conduct material testing horizontally or vertically. The large test furnace of the first equipment is 300 cm (width) ∗ 300 cm (height) ∗ 240 cm (depth) (Figure 1). The small test furnace of the second equipment is 120 cm (width) ∗ 120 cm (height) ∗ 120 cm (depth) (Figure 2). They both adopt the electronic ignition, and the control system used is the computer PID temperature controller. There are 8 burners in the large test furnace among which only 4 are switched on for the wall test. In the furnace, there are two thermocouples to, respectively, control the operation of 2 high-speed burners on two sides and other 7 thermocouples are to measure the temperature in the furnace. All thermocouples are inserted from the top of the test furnace. There are 4 burners in the small test furnace. When the wall is tested, only 2 burners which are close to the wall are opened. In the furnace, there are two thermocouples to, respectively, control the operation of 1 high-speed burner on two sides and other 2 thermocouples are to measure the temperature in the furnace. All thermocouples are inserted from the left side to right side of the test furnace. The ceramic wool is paved around and the top of the furnace wall of which maximum temperature is 1400°C and density is 240 kg/m^3. The furnace bottom is made by the adiabatic board of which thermal resistance is 1400°C and density is 1140 kg/m^3. The refractory mortar is applied in the gap and connection of adiabatic boards. The exterior body of the test furnace is made by steel plate and steel frame. At the back of the test furnace, there is an air outlet for exhaust air, and it is connected to the outdoor chimney. All the thermocouples are 10 cm away from the fire testing area of the specimen. The temperature in the furnace is measured by a K-type thermocouple of which specification conforms to the regulation of CNS 5534 [17] that the thermocouple shall possess property above 0.75 Grade. The thermocouple wire is covered by the heat-resistant stainless steel pipe of which the diameter is 6.35 mm

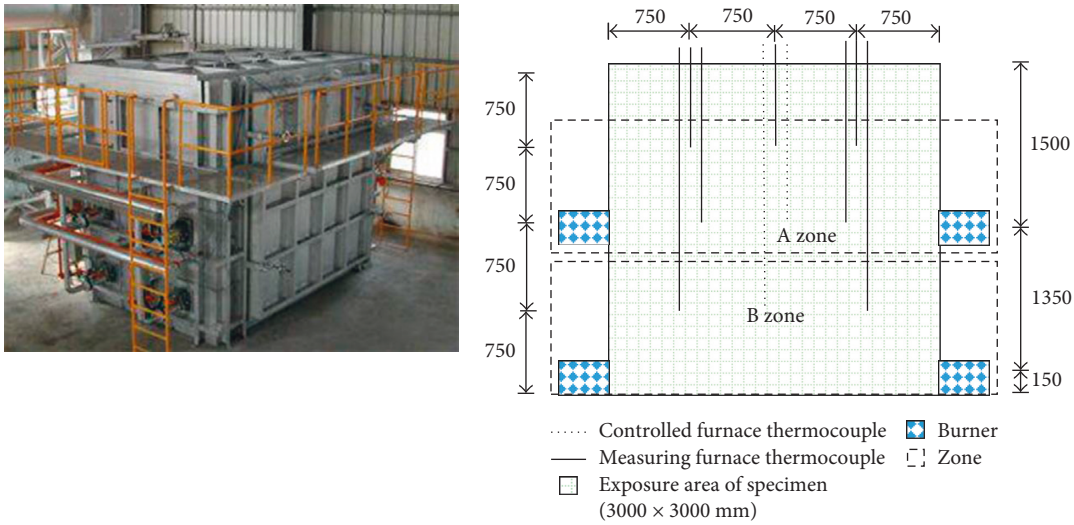

Figure 1: Full-size high-temperature furnace (inner size: 300 cm in width, 300 cm in height, and 240 cm in depth).

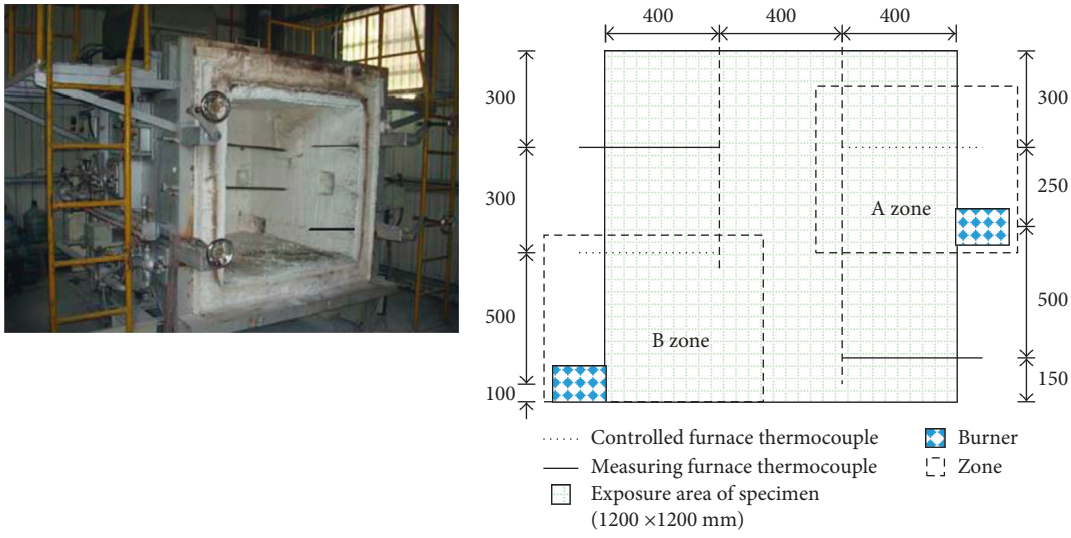

Figure 2: Small-size high-temperature furnace (inner size: 120 cm in width, 120 cm in height, and 120 cm in depth).

(16 gauge). In addition, the heat-resistant stainless steel pipe is placed in the insulated stainless steel pipe with an inner diameter of 14 mm and the front end is open and the hot junction of front end extrudes 25 mm. All the thermocouples in the furnace have been placed in the environment at a temperature of 1000°C for 1 hour [2] before the first use to increase the sensitivity of measuring the temperature, and the accuracy requirement is ±3%. All instrument signals are connected to the DS600 data recorder first, and DS600 processes and converses the signal to DC 100. At last, the data capture recorder converses the signal and outputs to the ThinkPad W540 laptop by a network cable. The data capture recorder is set to record once in every 6 seconds.

2.2. Test Specimens. The material used in the research is 9 mm calcium silicate board which is an erect blanking plate and fixed by a self-tapping screw. The self-tapping screw's diameter, length, and distance are 3.5 mm, 25.4 mm, and 250 mm, respectively. Its column is 65 × 35 × 0.6 mm C-shaped steel, and the upper and down channels are 67 × 25 × 0.6 mm C-shaped steel. The distance of the intermediate column is 406 mm, and the distance of the column away from two sides is 297 mm. The thickness of mineral wool is 50 mm, and a density of 60 kg/m^3 is applied to the material. For the size of the embedded socket, the external switch panel is 120 mm × 70 mm, and the internal junction box is 101 × 55 × 36 mm. There are two kinds of external switches. In Test 2, the material of the switch panel

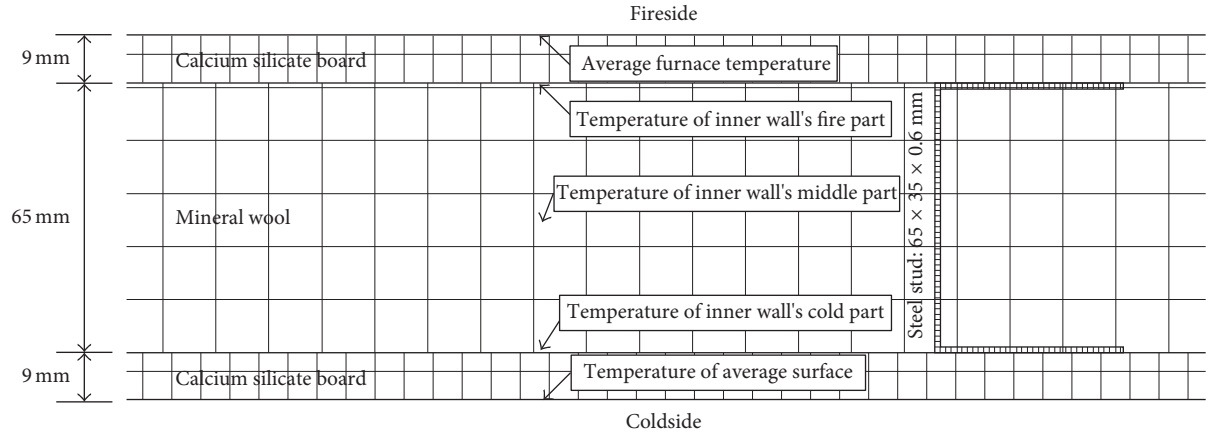

Figure 3: Cross section of the wall with indication of numerical modelling and the thermocouple position in Test 1.

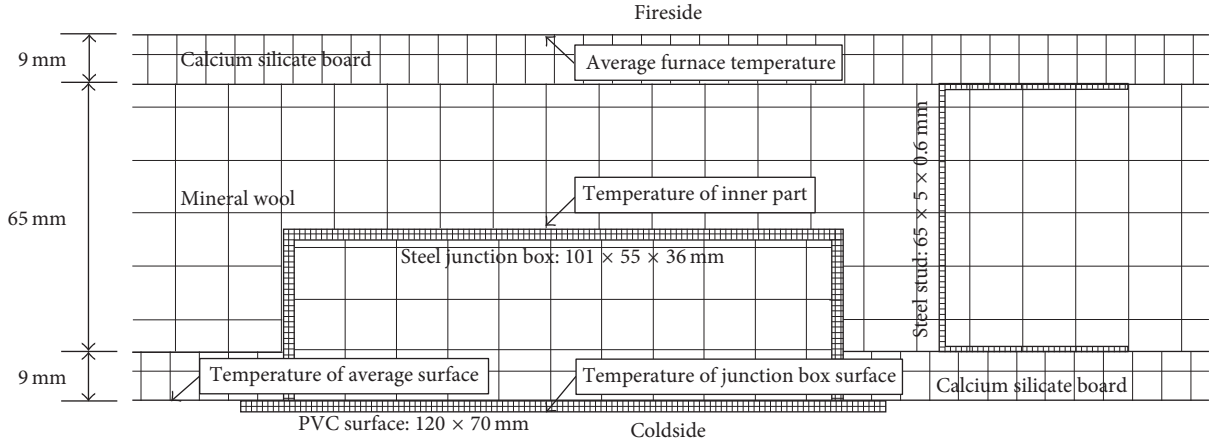

Figure 4: Cross section of the wall with indication of numerical modelling and the thermocouple position in Test 2.

is PVC (polyvinyl chloride), and the internal material is galvanizing steel box. In Test 3, the material of the external switch panel is steel, and the internal material is the galvanizing steel box. The junction box in Test 2 is not equipped with any reinforcement measures. Besides that the steel is selected in Test 3 as the material of the external panel, 9 mm calcium silicate board is added behind the junction box which is close to the fire source.

Three 60-minute standard heating tests were performed in the research. Test 1 is a standard test in which the specimen size is 3 m (height) × 3 m (width) and the density of fireproof cotton is 60 kg/m^3 as shown in Figure 3. Test 2 is a standard test with small high-temperature furnace in which the specimen size is 1 m (height) × 1 m (width) and the density of fireproof cotton is 60 kg/m^3. The socket junction box is embedded in the unexposed surface of the specimen. In addition, the material of the switch panel is PVC (polyvinyl chloride), and the internal material is the galvanizing steel box as shown in Figure 4. Test 3 is a test with small high-temperature furnace in which the specimen size is 1 m (height) × 1 m (width) and the density of fireproof cotton is 60 kg/m^3. The socket junction box is embedded in the unexposed surface of the specimen. In addition, the material of the switch panel is steel, and the internal material is the galvanizing steel box. A 9 mm calcium silicate board is added at the back of the box, as shown in Figure 5. Because there is no limit for the height that the socket junction box should be placed in the wall, this research expects to observe and simulate the most typical model in reality. In addition, according to the regulations of ISO 834-1 [2] that the weakness of the specimen shall be located in the center, the specimen of this research is 1 m (height) × 1 m (width) and the socket junction box is placed in the position 55 cm away from the ground. The furnace pressure is lower when it is more close to the bottom of the furnace. In short, the furnace pressure increases linearly as the height of the specimen increases. However, the furnace pressure is the negative pressure when it is 50 cm below the ground. As a result, the socket junction box is placed in the positive pressure position. As the test expects to verify the similarity of results of numerical modelling and test by Test 1, it takes the full-scale standard test of 3 m (height) × 3 m (width). The research expects to discuss the devastation that the embedded electronic junction box affects the components of wall, propose the reinforcement measures combining with the result of numerical modelling, and verify these measures through Test 2 and Test 3. As a result, it selects the test with small high-temperature furnace, and the size of the specimen is 1 m (height) × 1 m (width).

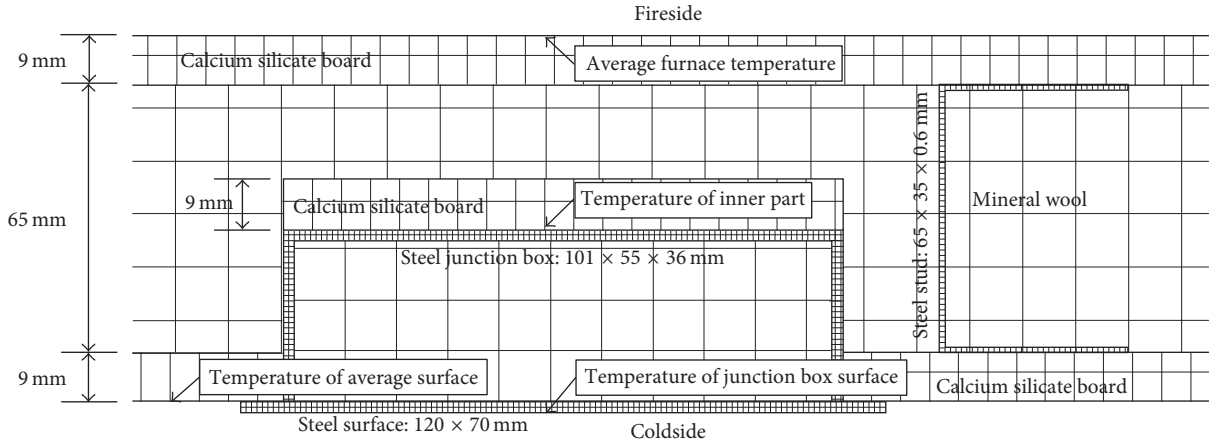

Figure 5: Cross section of the wall with indication of numerical modelling and the thermocouple position in Test 3.

2.3. Test Conditions. Test 1 follows the ISO 834-1 [2] standard. The size of the fire testing specimen is 3 m (height) × 3 m (width), and the zero pressure of the test furnace is at the height of 50 cm from the furnace bottom. As a result, according to the regulation of ISO 834-1 [2], 8 Pa should increase as the height increases every 1 m and the furnace pressure on the top of the specimen should not exceed 20 Pa; the standard heating curve of the test furnace is calculated using the following equation, and the furnace pressure measurement is recorded by a computer every 6 seconds:

$$T = 20 + 345 \times \log_{10}(8t + 1), \quad (1)$$

where T: average standard furnace temperature (°C) and t: time (min).

The heating temperature of Test 2 and Test 3 is adopted from the ISO 834-1 [2] standard heating curve, and the furnace pressure of the specimen is also set that the zero pressure is at the height of 50 cm from the furnace bottom. As a result, according to the regulation of ISO 834-1 [2], 8 Pa should increase as the height increases every 1 m and the furnace pressure on the top of the specimen is 4 Pa, and the pressure of the junction box is about 0.8 Pa.

2.4. Measurement and Recording of the Temperature of Standard Fire Test of Specimens. Test 1 sets 8 thermocouples on the unexposed surface of the specimen, as shown in Figure 6. According to the requirements of ISO 834-1 [2], temperature distribution is observed. Because it is required to compare the similarity of results of numerical modelling and tests and optimize the computer model, three measuring points are set in the middle layer of the wall and the measuring points are, respectively, in the position of 9 mm, 41 mm, and 74 mm, as shown in Figure 3. In Test 2 and Test 3, they, respectively, install the thermocouples on the unexposed surface of the specimens, as shown in Figure 7; four thermocouples are, respectively, located in the center of unexposed surface of the specimen, one in the center of wall, one on the panel of junction box, and another one in the center of mineral wool. The temperature measurement is recorded once in every 6 seconds by a computer, and it is recorded by photographs during the test.

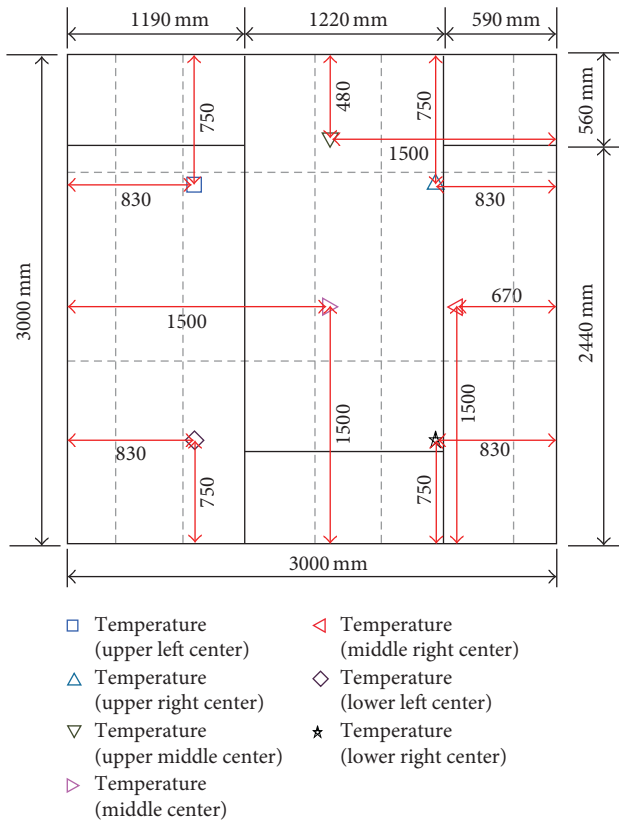

Figure 6: Test 1: the unexposed surface of the specimen and geometry of the thermocouple.

3. Numerical Modelling

3.1. General Modelling. In this study, numerical modelling is based on CFD technology for a series of computer simulation analysis, the use of software fluent to solve [18]. It can be roughly divided into three parts: preprocessing, solve, and postprocessing. Preprocessing mainly focuses on how to build the geometric model and mesh. This research needs to

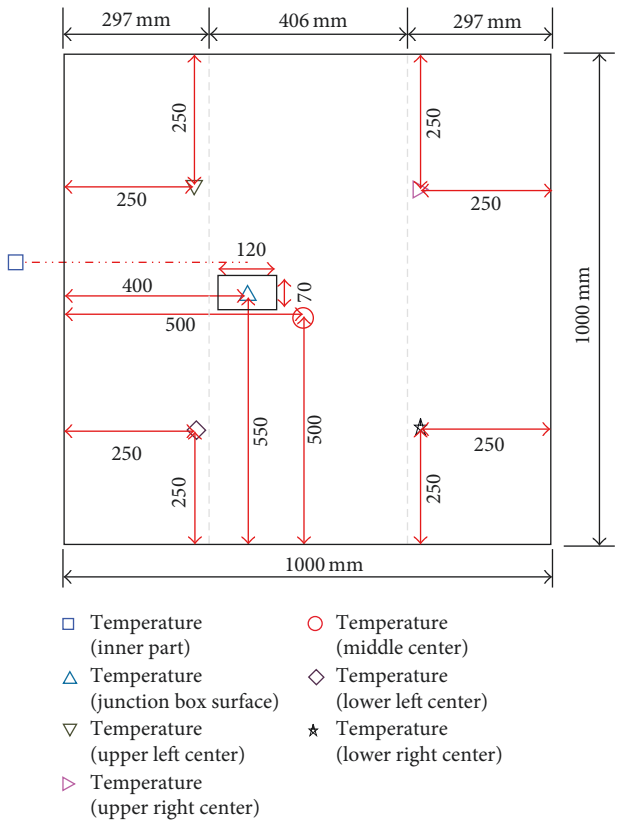

Figure 7: Test 2 and Test 3: the unexposed surface of the specimen and geometry of the thermocouple.

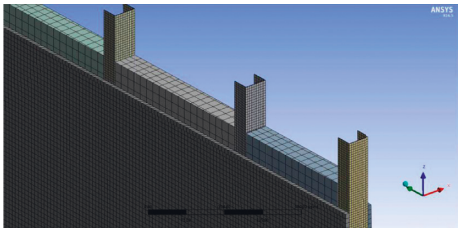

Figure 8: Numerical model of meshing.

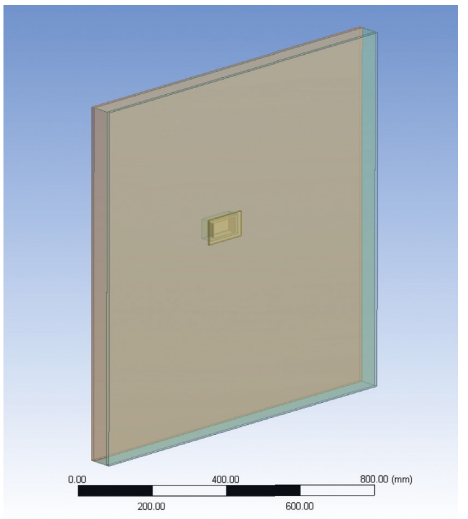

Figure 9: Numerical geometric model of wall embedded with the junction box.

get the computer model which matches the standard fire test result, so the geometric model is designed corresponding to the standard fire test of the specimen. The numerical modelling takes the finite element numerical analysis in which the principle is to divide the solution domains into several interrelated subdomain units, assume a proper approximate solution to every unit, deduce the general satisfied conditions of the domain, and work out the solution of the question. Therefore, it is necessary to build the geometric model and mesh it into several units. Based on the shape and size of building components, Test 1 meshes it by hexahedron, as shown in Figure 8. The meshing sizes of the calcium silicate board, steel stud, and fireproof cotton are $9 \times 9 \times 9$ mm, $0.6 \times 0.6 \times 5$ mm, and $25 \times 25 \times 25$ mm, respectively. The geometric model in Test 2 and Test 3 is added with the embedded junction box, as shown in Figure 9. In addition, this part is added to the meshing. The meshing size is $0.5 \times 0.5 \times 0.5$ mm, and the other part is the same as Test 1. Solve mainly includes how to set up the related material parameters, set boundary conditions, and select the mathematics model and calculation methods. Postprocessing aims to analyze the data solved by modelling.

3.2. Parameter Setting. The materials used in the test include steel, calcium silicate board, PVC, and mineral wool. The parameters involved in the modelling material are specific heat (J/kg°C), thermal conductivity (W/m°C), and density

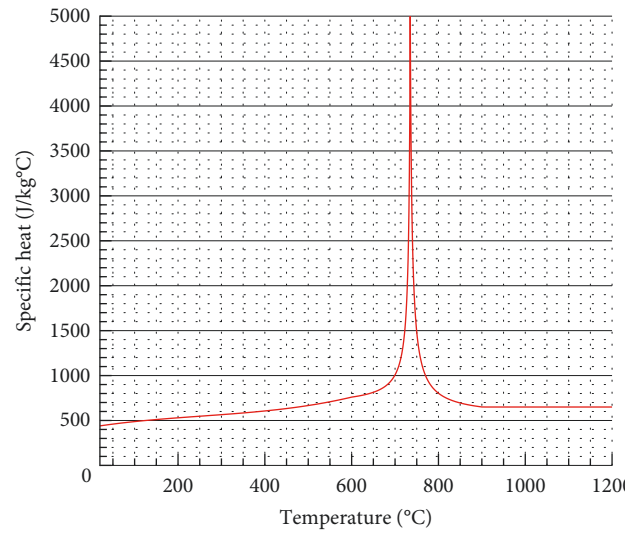

Figure 10: Specific heat for steel at elevated temperatures (BS EN 1993).

(kg/m^3). The parameters used in steel refer to the regulations of BS EN 1993 [19]. In addition, the specific heat of steel linearly increases as the temperature rises, as shown in Figure 10. The thermal conductivity of steel is 53.3 W/m°C when the temperature is 20°C, and it rises to 27.4 W/m°C

when the temperature is 800°C. However, the thermal conductivity is stable when the temperature is more than 800°C. The density of steel is 7850 kg/m^3. Walker and Pavía [20] performed research on the thermal performance of a series of insulation materials. According to their related data, the specific heat of the calcium silicate board is 819.4 J/kg°C. The regulation of GB/T 10699-1998 [21] stipulates the thermal conductivities of the calcium silicate board at various temperatures and other parameters. Its thermal conductivity is shown in the following equation, and the thermal conductivity of the calcium silicate board linearly increases as the temperature rises, as shown in Figure 11:

$$\lambda = \begin{cases} 0.0564 + 7.786 \times 10^{-5} \times t + 7.8571 \times 10^{-8} \times t^2 & (t \le 500^\circ\text{C}) \\ 0.0937 + 1.67397 \times 10^{-10} \times t^3 & (500 < t \le 800^\circ\text{C}), \\ 0.179 & (t > 800^\circ\text{C}) \end{cases} \quad (2)$$

where λ: thermal conductivity (W/m°C) and t: temperature (°C).

In this research, the PVC (polyvinyl chloride) panel of the junction box used in Test 2 conforms to the regulations of CNS 3142 [22]. According to the related researches made by Mansour et al. [23], the values of the specific heat, thermal conductivity, and density of PVC are 900 J/kg°C, 0.16 W/m°C, and 1380 kg/m^3, respectively. In this research made by Nassif et al. [15], it presents some material property parameters related to mineral wool. Combining the specifications of mineral wool used in this research, the specific heat, respectively, is 840 J/kg°C and thermal conductivity increases as the temperature rises [24], as shown in Table 1. The density of mineral wool is, respectively, 60 kg/m^3. The specific setting is shown as Table 2.

4. Results and Discussion

4.1. Test Results. The test time for Test 1 lasted 60 minutes. After 9 minutes of the test, trace smokes with abnormal smell burst out above the unexposed surface of the specimen and the seams of framework. At this time, all temperatures of measuring points obviously tend to rise (Figure 12). Until the 14th minute, the temperature of the measuring point on unexposed surface tends to decline until the 35th minute. From the 35th minute to the end, the temperatures rise all the time. The temperature of the inner wall's fire part rises rapidly after 9 minutes, and it slowly rises to the end after 22 minutes. At the end of test time, the temperature of the measuring point is 738.1°C. The temperature of the inner wall's middle part rises rapidly after the test begins till 9 minutes, and the rise begins to slow down towards the end after 38 minutes. At the end of test time, the temperature of the measuring point is 487.8°C. The situation of temperature of the inner wall's cold part is generally the same to that of the temperature of the side wall within the first 18 minutes. After that, the temperature gradually goes up to the end, and the final temperature is 316.5°C. At the 21st minute, a transverse crack appears on the upward side of the left board of the unexposed surface, and the crack extends to the center at 38th minute. When the test time is over, the temperature in the upper left center is the highest one (104.7°C) among temperatures on the unexposed surfaces, and the highest average temperature was 97.5°C (Figure 13), which does not exceed the stipulated fire resistance given in regulations of ISO 834-1 [2]. After the test, the integrity of the unexposed surface of the specimen is still good (Figure 14). Therefore, the specimen meets the demand of 60-minute fire resistance.

The test time of Test 2 lasted 60 minutes. After 6 minutes of the test, some smokes burst out and all temperatures of measuring points obviously tend to rise. Until the 37th minute, the temperatures of the thermocouple steadily increase, and the temperature junction box surface rises most sharply. It can be found that the embedded junction box has a great effect on the fire resistance of the metallic wall system. After that, the temperature significantly decreases and maintains around 40°C until the end of test. This is because the external panel of the junction box is PVC. According to the regulation of CNS 3142 [22], the softening temperature of PVC is not less than 73°C. The temperature of the thermocouple is higher than 100°C at the 28th minute, and the external panel of the junction box softens comprehensively (Figure 15) and falls out. This thermocouple is placed on the panel of the junction box, so the recorded temperature tends to plunge. Other temperatures of measuring points increase steadily. Among them, the temperature of the upper left center rises most significantly. This is because the furnace pressure is in a rising trend, and the temperature of the upper specimen is higher than that of the below specimen. The junction box is placed left-to-center, so the hot gas is released to the unexposed side from the weak surface after the weak surface is destroyed. After that, the hot gas rises rapidly making the temperature of the thermocouple higher than other temperatures. Until the 57.6th minute, the temperature of the upper left center is 207.8°C (Figure 16) and its initial temperature is 25°C, increasing by 182.8°C. According to ISO 834-1 [2], when the highest temperature of the unexposed surface is higher than the initial temperature by 180°C, it can be judged that the fire resistance is destroyed. After the test, the junction box panel on the unexposed surface of the specimen falls out, so the integrity is destroyed (Figure 17). Therefore, this specimen does not meet the demand of original 60 min fire resistance.

The test time of Test 3 lasted 60 minutes. After 6 minutes of the test, some smokes burst out and all temperatures of measuring points obviously tend to rise. After 15 minutes, the temperature of the inner part increases more obviously and the temperature is 463.4°C at the end of the test. All

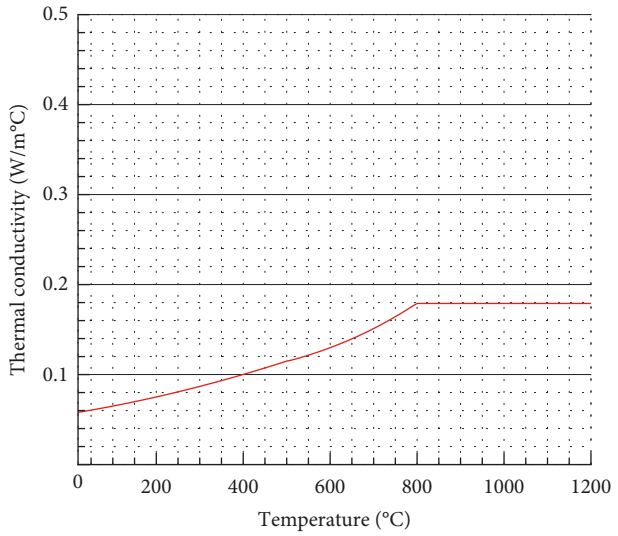

Figure 11: Thermal conductivity for the calcium silicate board at elevated temperatures.

Table 1: Thermal conductivity of the mineral wool.

Mineral wool					
Temperature (°C)	23.9	93	149	260	371
Thermal conductivity (W/m°C)	0.038	0.045	0.057	0.069	0.082

Table 2: Thermal properties.

Material	Specific heat (J/kg°C)	Thermal conductivity (W/m°C)	Density (kg/m^3)
Steel	According to Figure 10	20°C, 53.3 $T \geq 800$°C, 27.4	7850
Calcium silicate	819.4	According to (2)	1350
PVC	900	0.16	1380
Mineral wool	840	According to Table 1	60

temperatures steadily rise. From 20th to 30th minute, the temperatures rise more sharply. After that, they tend to be stable until the 48th minute. From the 48th minute, the rising range of the temperature becomes greater towards the end. Among the temperatures, the temperature of the junction box surface rises most obviously, followed by the temperature of the upper left center. It is because the junction box fire resistance performance is still weaker than the surrounding integrated wall although it has been strengthened. Therefore, the junction box temperature is higher than other places. At the end of test, the temperature of the junction box surface is highest on the unexposed surface which is 198.2°C (Figure 18). The initial temperature is 25°C, increasing by 173.2°C. The highest average temperature of all the measuring points is 136.5°C, increasing by 111.5°C. According to ISO 834-1 [2], the highest temperature rise of unexposed surfaces should not be higher than 180°C from the initial temperature and the

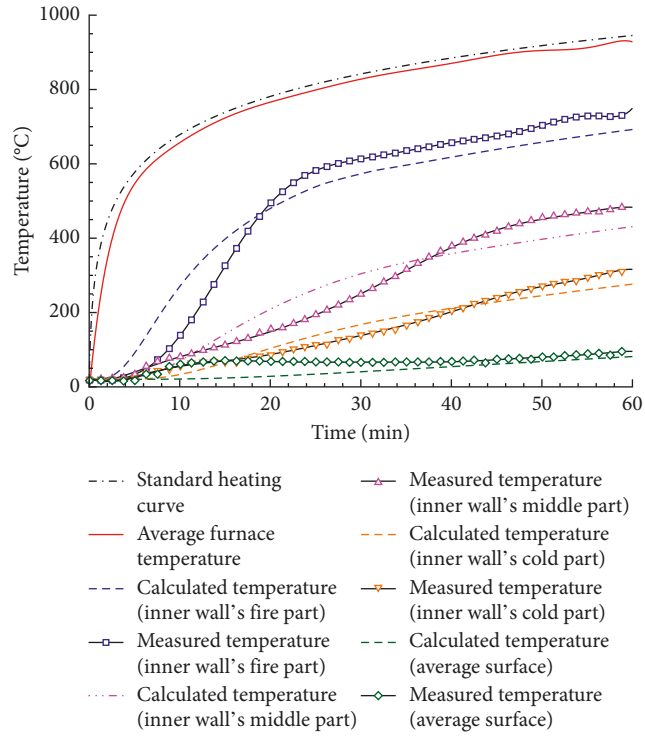

Figure 12: Measured temperatures compared to the calculated values in Test 1.

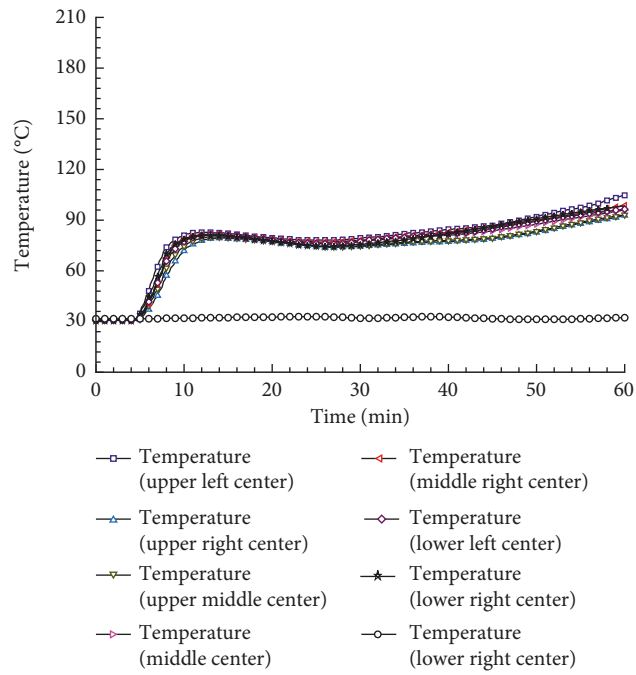

Figure 13: Time-temperature chart for the specimen in Test 1.

average temperature rise should not be higher than 140°C. During the test, these temperatures did not exceed the value given in the regulation of ISO 834-1 [2]. After the test, the integrity of unexposed surface of the specimen is still good (Figure 19). Therefore, the specimen meets the demand of 60-minute fire resistance.

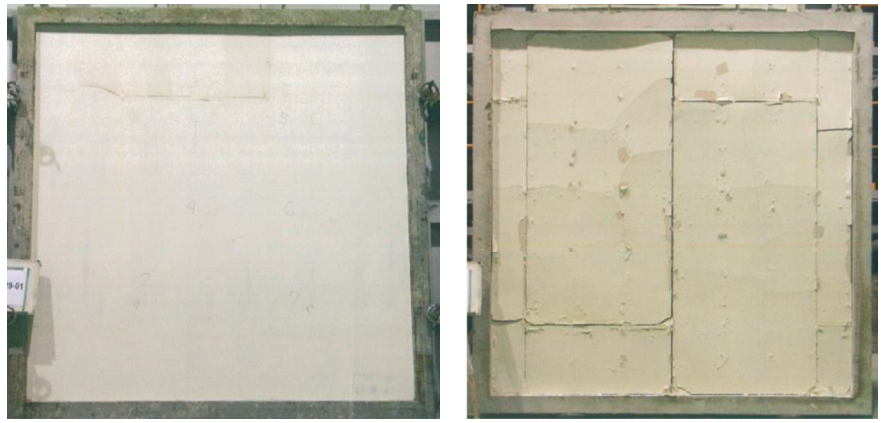

(a) (b)

Figure 14: The result of the specimen after 60 min standard fire test in Test 1. (a) Unexposed surface. (b) Exposed surface.

4.2. General Discussion. Test 1 is the full-scale standard test with 3 m (height) × 3 m (width), and its standard fire test specimen and measuring temperatures of CFD finite element numerical modelling are in accordance with the test. The results obtained by comparing numerical modelling and standard fire test are shown in Figure 12. The heating curve of the test furnace is in accordance with the modelling standard heating curve which shows that the standard fire test temperature confirms with the regulation of ISO 834-1 [2]. In the standard fire test, the temperature of the inner wall's fire part rises faster in the first 22 minutes of the test and rises slower from 22nd minute to 60th minute. Similarly, the heating curve of numerical modelling on this measuring point is relatively ideal, which is basically coincident with the escalating trend of this measuring point in the standard fire test. In the first 20 minutes, the temperature of the inner wall's middle part rises slower, and after that, it rises faster. It is because at the 21st minute, a transverse crack appears on the upward side of the left board of unexposed surface and causes the temperature to rise faster. Because the numerical modelling is in an ideal condition, the numerical modelling temperature on this point rises slowly and continuously, so there will be a curve alternating situation of temperature slope and solid test temperature slope. However, the overall escalating trends are highly coincident. The temperature of the inner wall's cold part is away from the fire source, so its temperature heating curve is gentler than previous two temperatures, and it is highly correlated to the numerical modelling temperature. In the standard fire test, trace smokes with abnormal smell burst out above the unexposed surface of the specimen and the seams of framework at the 9th minute, so the average temperature on the unexposed surface greatly rises but tends to rise slower, corresponding with the numerical modelling temperature. Through the comparison, it can be found that the temperature ascending curves of different measuring points of numerically predicted values are highly correlated with the data of all temperature measuring points in the standard fire test in 60 minutes.

From Test 1, it can be found that the specimen without the junction box can meet the demand of 1-hour fire resistance and the CFD numerical modelling result is highly correlated with the standard fire test. Test 2 expects to focus on exploring the effect of the specimen with the embedded junction box on the fire resistance and whether its related numerical modelling has correlation with the standard fire test result. Therefore, in Test 2, the specimen size is designed to be 1.0 m (height) × 1.0 m (width) and the junction box is embedded into the unexposed surface. The external panel of the junction box is PVC (polyvinyl chloride). In addition, the numerical model is added to the junction box, including the construction of the internal box and the external panel. The comparison of the standard fire test result and the numerical modelling result is shown in Figure 20. In the figure, it can be seen that the temperature heating curve of the test high-temperature furnace is very close to the standard heating curve in 60 minutes. It shows that the temperature of the burning furnace in the standard fire test meets the demand of ISO 834-1 [2]. The temperature value of the inner part in the standard fire test has limited difference from the numerical modelling temperature value on

Figure 15: The external panel of the junction box softens at 28th minute in Test 2.

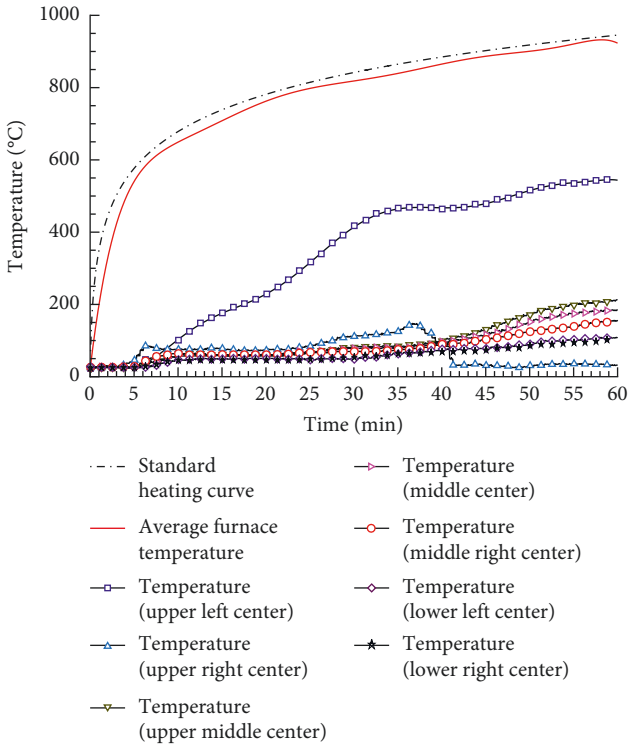

Figure 16: Time-temperature chart for the specimen in Test 2.

Figure 17: The result of the specimen after the 60 min standard fire test in Test 2.

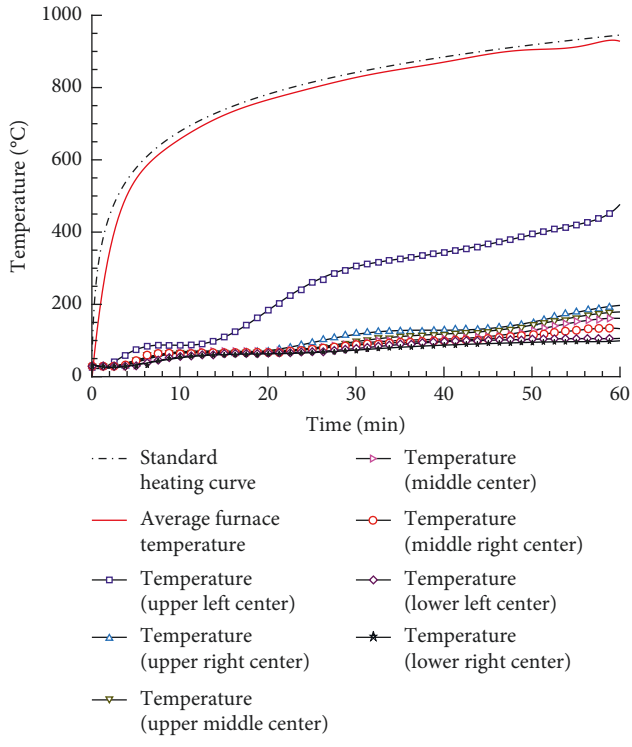

Figure 18: Time-temperature chart for the specimen in Test 3.

Figure 19: The result of the specimen after the 60 min standard fire test in Test 3.

this point, and their escalating trends are basically corresponding and highly correlated. The actual temperature of the junction box surface is highly correlated with the temperature of the calculated junction box surface from test beginning to 37th minutes. After that, the test recorded temperatures dramatically reduce until the end of the test. This is because the external panel of the junction box is PVC. According to the regulation of CNS 3142 [22] that the softening temperature of PVC is not less than 73°C, the temperature of the thermocouple is more than 100°C at 28th minutes and the external panel of the junction box softens comprehensively and falls out at 37th minute. As a result, the test temperature dramatically reduces after that, which is obviously different from the calculated temperature after 37 minutes. The average surface temperature and calculated average surface temperature's escalating trends are highly correlated. By comparison, it can be found that the standard fire test result is in accordance with the numerical modelling result in Test 2. Through the observation of the standard fire test and prediction of numerical modelling, it can be seen that after the junction box is embedded in the wall member, it will cause damage in two aspects, resulting in the

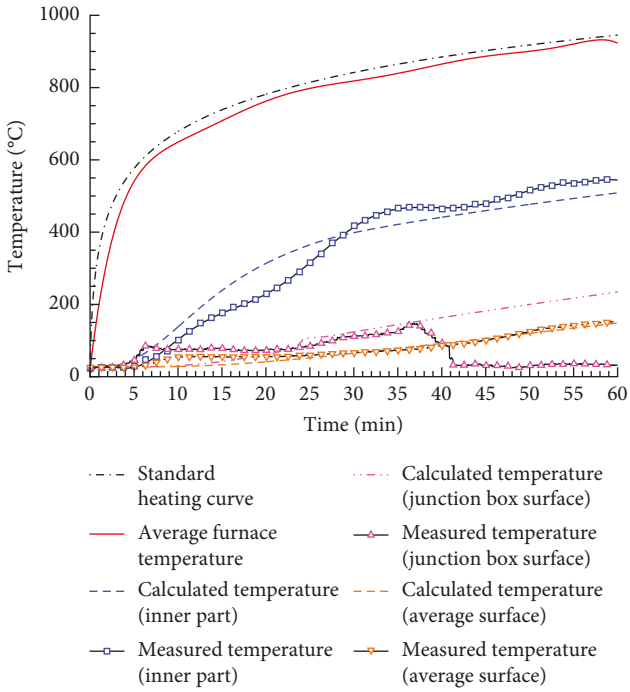

Figure 20: Measured temperatures compared to the calculated values in Test 2.

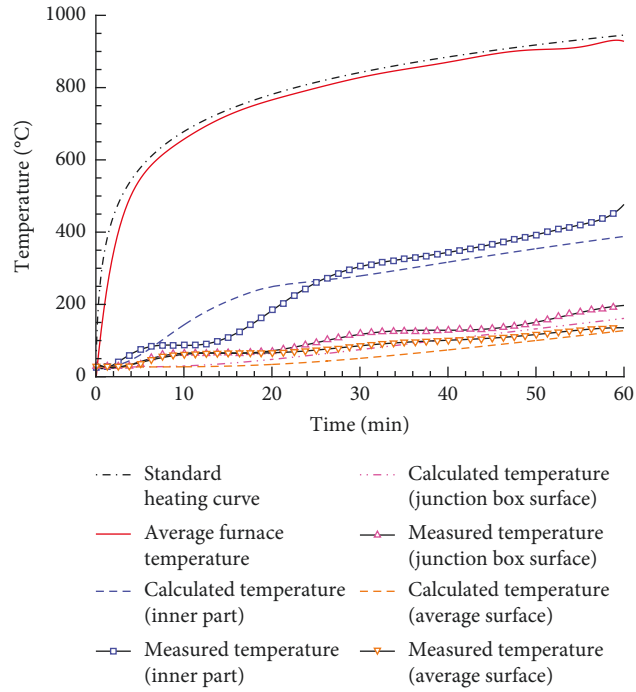

Figure 21: Measured temperatures compared to the calculated values in Test 3.

component failing to reach the original 1-hour fire resistance limitation. First, the material of the junction box is metal and its thermal conductivity is much higher than that of mineral wool and calcium silicate board, so the heat transmits to the unexposed surface faster. Second, the external panel material of the junction box is PVC and it begins to soften when the temperature is at 80~100°C. When the temperature rises, the panel falls out and the external junction box exposes. The material of the junction box is metal and it has high thermal conductivity, so it destroys the fire resistance of component.

The result of Test 2 shows that the position of the embedded junction box has a higher temperature than other parts and that the PVC junction box panel softens and falls out in heat which destroys the integrity of wall. According to above weaknesses, Test 3 proposes related reinforcement measures. Considering the density of the calcium silicate board as 1350 kg/m^3 and the mineral wool as 60 kg/m^3, the fire resistance performance of the calcium silicate board is much better than that of the mineral wool under the same thickness, although its thermal conductivity is slightly higher than the mineral wool. Therefore, a reasonable reinforcement measure is adding the calcium silicate board to the back of junction box and changing the PVC material to metal material. After these adjustments, modify the numerical models and parameters. When the modelling result meets the demand of 1-hour fire resistance, the standard fire test can be processed to verify. The final comparison of the standard fire test result and numerical modelling result is shown in Figure 21. According to the regulation of GB/T 10699-1998 [21], the water content of the calcium silicate board is not more than 10%. Therefore, the board contains certain water. The specific heat of water is higher and the heating temperature variation is not obvious, so the temperature of the inner part of the standard fire test at the beginning of heating is lower than the numerical modelling temperature. However, after the water evaporates completely, the temperature rapidly rises, which is highly correlated with the numerical modelling temperature. As shown in Figure 21, it can be seen that the temperature of the junction box surface is still higher than the temperature of the average surface. Although two aspects on the weakness are reinforced, it is still limited by the material and it cannot be completely identical with the original wall. The temperature of the junction box surface is the highest temperature on unexposed surface, but it can meet the demand of 1-hour fire resistance. The final result of the standard fire test in Test 2 shows that the temperature of the average surface is 153.0°C. When the standard fire test of Test 3 is over, this temperature is 138.2°C, reducing by 14.8°C. Because the panel falls out at after 37 minutes, the measurement of the temperature of the junction box surface in Test 2 distorts. The final temperature of the junction box surface of the standard fire test in Test 3 is 186.2°C, conforming to the standard of ISO 834-1 [2]. When the numerical modelling of Test 2 is over, the temperature of the average surface is 148.6°C and temperature of the junction box surface is 234.2°C. When the numerical modelling of Test 3 is over, the temperatures are, respectively, 127.5°C and 161.3°C, reducing by 21.1°C and 72.9°C, respectively. It can be seen that compared with Test 2, the temperatures on unexposed surface obviously reduce after reinforcement in Test 3 and the temperature of the junction box surface reduces most

significantly. However, in numerical modelling and standard fire test, the metallic-framework walls with embedded junction boxes after reinforcement in Test 3 can meet the demand of 1-hour fire resistance.

This is an innovative research. It is the first time to put forward the quantitative research on influence of embedded junction box on fire resistance of metal frame walls and analyze the weakness. In addition, it proposes effective reinforcement aiming at the weakness. After the reinforcement, the wall meets the demand of 1-hour fire resistance when the metallic-framework wall is embedded with the junction box. During the process, it successfully builds the CFD numerical models which is corresponding with the specimens, successfully predicts the effect of reinforcement by modified model parameters, and verifies it in the following standard fire test. This research not only systematically analyzes the metallic-framework wall with the embedded junction box and proposes effective reinforcement measures but also predicts them by CFD numerical modelling and verifies them successfully in the test. It is proved that the pattern of numerical modelling before the standard fire test is effective. Similar patterns can be applied to other researches on the wall systems and that can greatly save the cost of the test. Before the test, the numerical modelling can be processed to work out the predicted results. When the predicted result is satisfying, the standard fire test can be processed to verify.

5. Conclusions

(1) When the junction box is embedded into the metallic wall, the fire resistance of wall may be damaged because the metal junction box has a larger thermal conductivity and transfers the heat faster, while the PVC panel of the junction box softens in heat.

(2) The result of numerical modelling predicting the temperature by finite element is highly correlated to the result of standard fire test.

(3) After reinforcement, the temperature of the junction box surface decreases most significantly, and in Test 3, it reduces by 72.9°C when compared to Test 2.

(4) Adding the calcium silicate board to the back of the junction box and using the metal panel instead of the PVC panel can reinforce the original weakness effectively and help the metallic wall with the embedded junction box to meet the demand of 1-hour fire resistance.

(5) Making use of the finite element numerical modelling method to predict the test result is an effective way. It can be applied to other related fire prevention research and product development.

Conflicts of Interest

The authors declare that there are no conflicts of interest regarding the publication of this paper.

Acknowledgments

This work was supported by the CABR Application Technology Research Project: Key Technology of Smoke Control for Ultra Thin and Tall Atriums (no. 20150111330730049).

References

[1] NFPA 251, *Standard Methods of Tests of Fire Resistance of Building Construction and Material*, National Fire Protection Association, Quincy, MA, USA, 2006.

[2] ISO 834-1, *Fire-Resistance Tests-Elements of Building Construction: Part 1: General Requirements*, International Organization for Standardization, Geneva, Switzerland, 1999.

[3] JIS A 1304, *Method of Fire Resistance Test for Structural Parts of Buildings*, Japan Standards Association, Tokyo, Japan, 1994.

[4] CNS 12514, *Method of Fire Resistance Test for Structural Parts of Building*, Taiwan Standard, 2005.

[5] UL 263, *Fire Tests of Building Construction and Materials*, UL, Northbrook, IL, USA, 1997.

[6] BS 476-22, *Fire Tests on Building Materials and Structures. Methods for Determination of the Fire Resistance of Non-Loadbearing Elements of Construction*, BSI Group, London, UK, 1987.

[7] CNS 14652, *Glossary of Terms Used for Fire Protection in Building-Fire Test*, Taiwan Standard, 2008.

[8] S.-H. Lin, C.-L. Pan, and W.-T. Hsu, "Monotonic and cyclic loading tests for cold-formed steel wall frames sheathed with calcium silicate board," *Thin-Walled Structures*, vol. 74, pp. 49–58, 2014.

[9] M.-C. Ho and M.-J. Tsai, "Relative importance of fire resistance performance of partition walls," *Journal of Marine Science and Technology*, vol. 18, no. 3, pp. 430–434, 2010.

[10] M. Nithyadharan and V. Kalyanaraman, "Experimental study of screw connections in CFS-calcium silicate board wall panels," *Thin-Walled Structures*, vol. 49, no. 6, pp. 724–731, 2011.

[11] Y.-J. Chuang, W.-T. Wu, H.-Y. Chen, C.-H. Tang, and C.-Y. Lin, "Experimental investigation of fire wall insulation during a standard furnace fire test with different initial ambient air temperatures," *Journal of Applied Fire Science*, vol. 15, no. 1, pp. 41–55, 2006.

[12] I. Maruyama, G. Igarashi, Y. Nishioka, and Y. Tanigawa, "Carbonation and fastening strength deterioration of calcium silicate board: analysis of materials collected from a ceiling collapse accident," *Journal of Structural and Construction Engineering*, vol. 78, no. 689, pp. 1203–1208, 2013.

[13] P. C. R. Collier and A. H. Buchanan, "Fire resistance of lightweight timber framed walls," *Fire Technology*, vol. 38, no. 2, pp. 125–145, 2002.

[14] C. T. Do, D. P. Bentz, and P. E. Stutzman, "Microstructure and thermal conductivity of hydrated calcium silicate board materials," *Journal of Building Physics*, vol. 31, no. 1, pp. 55–67, 2007.

[15] A. Y. Nassif, I. Yoshitake, and A. Allam, "Full-scale fire testing and numerical modelling of the transient thermo-mechanical behaviour of steel-stud gypsum board partitionwalls," *Construction and Building Materials*, vol. 59, pp. 51–61, 2014.

[16] Y. Wang, Y.-J. Chuang, and C.-Y. Lin, "The performance of calcium silicate board partition fireproof drywall assembly with junction box under fire," *Advances in Materials Science and Engineering*, vol. 2015, Article ID 642061, 12 pages, 2015.

[17] CNS 5534, *"Thermocuples," Part 4: General Structural Matters*, Taiwan Standard, 1982.

[18] W. Yinuo, *The Standard Fire Testing and Numerical Modelling of the Behavior of Calcium Silicate Board Light Partition Wall Assembly with Junction Box*, Ph.D. thesis, National Taiwan University of Science and Technology, Taipei, Taiwan, 2018.

[19] BS EN 1993-1-2, *Eurocode 3: Design of Steel Structures—Part 1–2: General Rules Structural Fire Design*, BSI Group, London, UK, 2005.

[20] R. Walker and S. Pavía, "Thermal performance of a selection of insulation materials suitable for historic buildings," *Building and Environment*, vol. 94, pp. 155–165, 2015.

[21] GB/T 10699-1998, *Calcium Silicate Insulation, Part 5: Technical Requirements for Physical Performance*, China Standard, 1998.

[22] CNS 3142, *Polyvinyl Chloride Board, Part 3: General Quality*, Taiwan Standard, 2013.

[23] S. A. Mansour, M. E. Al-Ghoury, E. Shalaan, M. H. I. El Eraki, and E. M. Abdel-Bary, "Thermal properties of graphite-loaded nitrile rubber/poly(vinyl chloride) blends," *Journal of Applied Polymer Science*, vol. 116, no. 6, pp. 3171–3177, 2010.

[24] H. Kim, D. Park, E. S. Park, and H. M. Kim, "Numerical modeling and optimization of an insulation system for underground thermal energy storage," *Applied Thermal Engineering*, vol. 91, pp. 687–693, 2015.